Journal of
Composites Science

MDPI

Review

Three-Dimensional Printing of Polymer Composites: Manufacturing and Mechanics

Ryan Bernardy and Yingtao Liu *

School of Aerospace and Mechanical Engineering, The University of Oklahoma, Norman, OK 73019, USA; ryan.c.bernardy-1@ou.edu
* Correspondence: yingtao@ou.edu

Abstract: Polymers have been heavily used in manufacturing for decades, and with their use, improvements in the desired materials via composite materials utilizing a polymer matrix have been commonplace. Naturally, the increase in polymer additive manufacturing has come with an increase in interest in additively manufacturing polymer composites. This paper primarily covers the fused deposition modeling (FDM) method, ultraviolet (UV)-cured resin methods, multiple resin printing, and embedded sensors associated with additive manufacturing. In particular, the manufacturing and subsequent effect on material properties compared to unreinforced and unmodified 3D-printed polymers, the tradeoffs required in doing so, and the mechanisms behind these effects are discussed. The manufacturing methodology used or developed and the mechanisms behind these selections are discussed along with insights that could be gathered from material property effects seen across different studies. The mechanisms discussed also focus on the mechanisms between the different materials comprising the composite produced.

Keywords: fused deposition modeling; direct ink writing; discontinuous fiber; additive; manufacturing; continuous fiber; composite; reinforced; materials

check for updates

Academic Editor: Yuan Chen

Received: 13 November 2024
Revised: 3 January 2025
Accepted: 10 January 2025
Published: 12 January 2025

Citation: Bernardy, R.; Liu, Y. Three-Dimensional Printing of Polymer Composites: Manufacturing and Mechanics. *J. Compos. Sci.* **2025**, *9*, 33. https://doi.org/10.3390/jcs9010033

Copyright: © 2025 by the authors. Licensee MDPI, Basel, Switzerland. This article is an open access article distributed under the terms and conditions of the Creative Commons Attribution (CC BY) license (https://creativecommons.org/licenses/by/4.0/).

1. Introduction

Rapid innovations in additive manufacturing have led to a wide variety of advances across the encompassed fields as more applications of the developed technologies have been found. This leads to an ever-growing list of topics that those working in the related industries may encounter or otherwise find useful for application to their own specialty. A review of advancements and research in select subsections of composites produced utilizing additive manufacturing techniques can assist in staying aware of general trends for possible utilization in other fields.

A deeper understanding of why these composites work in the manner that they do is beneficial to people in industry as there is more nuance to how additively manufactured composites work compared to simply being reinforced isotropic matrix in an anisotropic arrangement composites. An overview of different additively manufactured composites in the context of the research performed as well as how it was performed, followed by the outcomes and a discussion that explains why the research was performed, is intended to help the reader further their knowledge.

This literature review is intended to cover the mechanics behind how these composites work and the manufacturing involved in fiber reinforcement of fused deposition modeling (FDM) printing, reinforcement of resin printing, multiple resin printing, and embedded sensors for composites made with additive manufacturing. There are other areas of composite additive manufacturing; however, these areas cover the core aspects of how common

reinforcements and secondary materials interact and compliment their primary materials in addition to how differing materials are often manufactured as one.

1.1. Backgrounds

1.1.1. FDM

In FDM 3D printing, stock filament material is extruded through a heating nozzle onto a build surface to continually add material as a bead of material in a programmed pattern, layer by layer, until the print is finished as a model ready for final post-processing into the end product. This is accomplished through CNC (computer numerical control) machines, similar to what is seen with traditional milling but utilizing an FDM toolhead for depositing materials (displayed in Figure 1) instead of a toolhead for removing materials. These machines utilize CAM (computer-aided manufacturing) software, commonly referred to as a "slicer", for turning digital models into a usable machine program. The materials, operating time, post-processing, design and slicing time, and machine electricity are all factors in the cost and requirements of producing usable products from these machines, and the effects on these factors are primarily what is referred to when discussing tradeoffs between reinforcement methods when analyzing advantages and disadvantages of reinforcement.

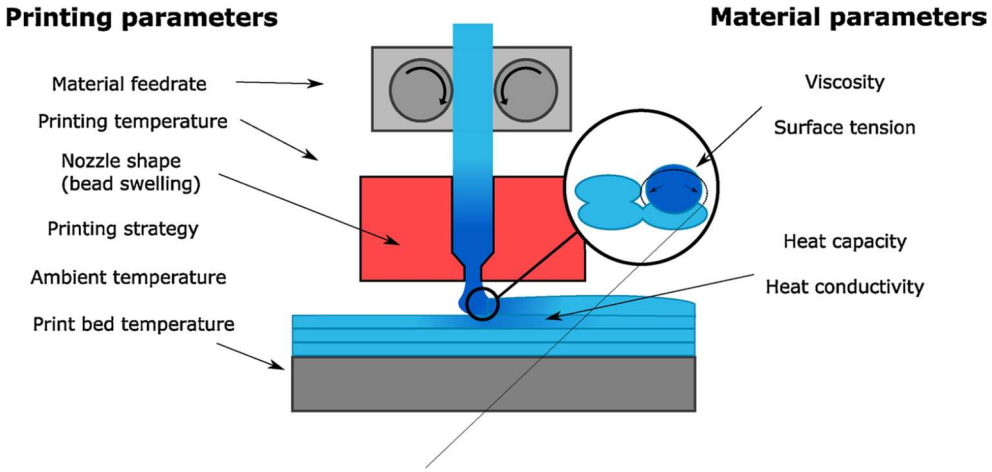

Figure 1. Diagram displaying FDM printing technique and associated variables [1].

There is a large difference in the processing, costs, and improvements between continuous and discontinuous fibers; however, both have been areas of research interest as both have applications in performance enhancement. The primary difference between the two types of fiber reinforcement is the length of the reinforcing fiber; continuous fiber reinforcement refers to fibers that are considered long enough to successfully transfer load to the next fibers when aligned along the stress direction, whereas discontinuous fibers are typically unaligned and short enough that they do not fully transfer load through the matrix into aligned fibers. When selecting studies for this review, there was an intentional choice to look for studies which used Markforged's continuous fiber reinforcement, with the assumption that samples produced with the same proprietary equipment and material ecosystem will be similar enough for comparison, so that tested and observed qualities can be compared despite not having been tested within the same study.

1.1.2. Resin 3D Printing

Thermoset resins can also be additively manufactured, with the most common methods involving a (UV) light curing method so that selectively applied UV lights can cause a solidified pattern which is typically layered until the desired 3D shape is printed. This is typically performed within a vat of resin and involves post-processing for removing excess

resin and a final cure cycle. These polymers are also reinforced with both continuous and discontinuous fibers, with many additional articles covering silver or other biocompatibility additives. Additional methods of resin printing involve depositing then curing the resin, with a small number of articles discussing the use of resin deposited with a machine similar to an inkjet printer for depositing a composite of different thermoset polymers.

The primary difference between thermoset resins used in UV curing and thermoplastic resins is that the UV resins undergo a crosslinking which causes the tangling of the polymers to require a higher thermal energy content to facilitate molecular movement than the energy required to cause chemical decomposition; therefore, thermoset resins will burn first and cannot melt for reshaping as thermoplastic polymers can. This leads to drastically different processing methods for manufacturing and differing utilizations outside of 3D printing, which some of the research covered mentions or considers in testing, such as adhesion bond strength for use in repair adhesives.

1.1.3. Traditional Reinforced Composite Background

The term "composites" commonly refers to either continuous fiber-reinforced thermoset resins or discontinuously reinforced thermoplastic resins, although the term includes all materials composed of multiple different materials which are distinctly separate within the composite material. Much of the research covered references traditionally manufactured composites as they are utilized heavily in industry for high-performance materials.

Traditionally manufactured continuous fiber composites are typically made with layers of continuous fiber in a woven or unidirectional pattern which are reinforced with a polymer matrix, commonly thermoset resins, but thermoplastics are also utilized. The traditionally manufactured composites typically use pre-impregnated fibers made by wetting the fibers with resins utilizing solvents or dry fibers using either vacuum or pressure to force melted or uncured resin into the fibers. Traditionally manufactured discontinuous fiber composites are manufactured in similar manner to traditionally manufactured thermoplastic polymers, as discontinuous fibers are typically reinforcements to thermoplastic polymer matrices.

2. Notable Techniques

2.1. Fiber-Reinforced FDM

All reviewed reinforced FDM articles utilized tensile samples, with various studies also performing flexural and shear testing. The tensile bars were typically differing types and patterns of fiber infill or discontinuous fiber reinforcement; several studies also performed an analysis of the breakages with a scanning electron microscope (SEM). There was a study comparing performance to predict performance based on already developed predictable models. The rest of this section summarizes the methodology of each reviewed article as it pertains to this report. Table 1 provides a brief overview of the differing reinforcements being added to their respective matrix's and the purpose those matrix's are being modified for.

Mohammadizadeh et al. [2] used printed samples with continuous fiber reinforcement of varying infill patterns and fiber reinforcement types which were tested for ASTM D638 tensile, ASTM E606 fatigue, and ASTM D2990 creep mechanical properties and then analyzed with an SEM for microstructure observation. The samples were produced with a Markforged Mark 2 printer, which utilizes a dual print head with a specialized nozzle and cutting mechanism for depositing a continuous strand of fiber within a matrix along the toolpath of the print.

Estakhrianhaghighi et al. [3] printed samples with varying percentages of discontinuous wood fiber infill in a polylactic acid (PLA) matrix and tested for ASTM D638 tensile strength and thermal conductivity followed by using an SEM for analyzing the fiber breaks.

The fiber reinforcement was mixed into the matrix by producing the filament feedstock from a PLA powder and sieved ground wood; this is also how the percentage of wood fiber was controlled with multiple batches of differing fiber to matrix ratios used to make the feedstock.

The experiment performed by Blok et al. [1] compared continuous and discontinuous fiber reinforcement with very similar polyamide polymer matrix selection. The continuous fiber prints were performed on a Markforged Mark One, with the discontinuous prints performed on a Lulzbot. These samples were tested for their ASTM D3039 (continuous) and ASTM D638 (discontinuous) tensile, ASTM D7264 flexural, and ASTM D3518 shear strengths.

Zhang et al. [4] focused on attempting to increase the fiber fraction of continuous fiber-reinforced 3D-printed polymers. During this research, they attempted to utilize a powdered epoxy for traditional composite vacuum bag curing as a post-processing step in order to increase the wettability of the fiber, thus decreasing the void content. These samples were compared to continuous fiber prints produced on a Markforged printer. The testing performed was ASTM D3039 tensile tests and included an ASTM D5766 open hole test with a drilled sample of traditionally manufactured continuous fiber and the additively manufactured sample having reinforcement placed around the hole in the printed sample.

Elastic properties were investigated by Abadi et al. [5], with ASTM D3039 tensile bar testing accompanied by strain gauges to verify the strain measurement recorded. The samples were produced from a Markforged Mark One printer with three samples each of carbon-, glass-, and Kevlar fiber-reinforced nylon; these were not produced with the same fiber direction in each layer, and the stacking sequence for each layer and both matrix and fiber directions are listed in the article. The experimental results were compared to finite element and volume average stiffness analysis methods.

2.2. Resin

2.2.1. Reinforced Resin

The resin articles had a common theme of investigating fiber direction and factors affecting void content and reinforcement wetting. Comparisons to expectations in traditional composites were common, with many utilizing models to describe and predict test results that were based on traditional composite models. The methods for manufacturing were a particular focus as there is significantly more variation available than what is found in FDM methods.

A resorcinol-based epoxy was formulated for UV curing and reinforced with glass, nylon, and polyester fibers by Prashil et al. [6] which were then analyzed for rheological properties before printing samples for comparison, characterizing the composites. The article details the formulation for producing the resin which was mixed with the different fibers and molded into samples under UV exposure, which were washed in isopropyl alcohol (IPA) and post-cured with UV in the same manner in which a resin print is post-processed. These samples underwent Fourier transform infrared analysis, C nuclear magnetic resonance analysis, viscosity measurement, ASTM D2240 Shore D hardness testing, gel content estimation, ASTM D570 water absorption testing, ASTM D543 chemical resistance testing, tensile testing, differential scanning calorimetry for the glass transition temperature, thermogravimetric analysis for thermal degradation, and microscope analysis for surface morphology.

Numerical analysis is the method utilized by Hofstatter et al. [7] for describing fiber orientation within vat photopolymerization printing. This analysis was performed for both the options for build plate orientation, printing on top of a plate moving vertically downwards and on the bottom of both a rectangular and circular plate moving vertically

upwards, and included a variation with a perforated build plate in the applicable upper plate moving downwards.

Khatua et al. [8] utilized a separate robot for placing and orienting fibers across a photopolymer resin vat utilizing a UV projector for embedding fibers into top-down resin prints. This process is demonstrated with several small cylinders showing variability in how the fibers can be placed and oriented and then demonstrated by printing models of naturally occurring fiber-reinforced items with continuous carbon fiber utilized along the fibers to model peanut shells and a leaf. The prints are post-processed with an IPA wash followed by a cure cycle. The intent is to utilize naturally occurring fiber orientations and directions with the belief that they are already optimized for compressive strength in the complex shape used.

Glass bead reinforcement was investigated by Gerbroodbar et al. [9] by mixing glass beads pre-coated with a UV resin into a printing UV resin. There is an in-depth description of the cleaning and preparation required to properly coat the beads to achieve proper adhesion to the matrix during printing. Samples were produced and tested for ASTM D790 flexural and ASTM D695 compression properties; then, SEM analysis was performed to assess breakages.

Idrees et al. [10] focused on a different aspect of fiber-reinforced composites, with the stiffness being a secondary consideration to the overall composite strength; the method of strengthening investigated is called "resin-rich layers", wherein layers without reinforcement are added in attempt to obtain the strength of the reinforcement without the increased brittle behavior found in higher fiber volume composites, causing a reduction in strength. During this experiment, fiber layers were made by adding wetted mats of fiberglass (displayed in Figure 2) into the vat of a digital light processing (DLP) bottom-up resin printer with unreinforced layers added to control the fiber content with exclusively resin layers between mats in an attempt to preserve plastic behaviors between reinforcement. Tensile (ASTM D3039), flexural (ASTM D7264), shear (ASTM D2344), and interlaminar fracture toughness (ASTM D5528, ASTM D7905) samples were fabricated and post-processed using a curing cycle, followed by polishing to remove any protruding fibers from the composite.

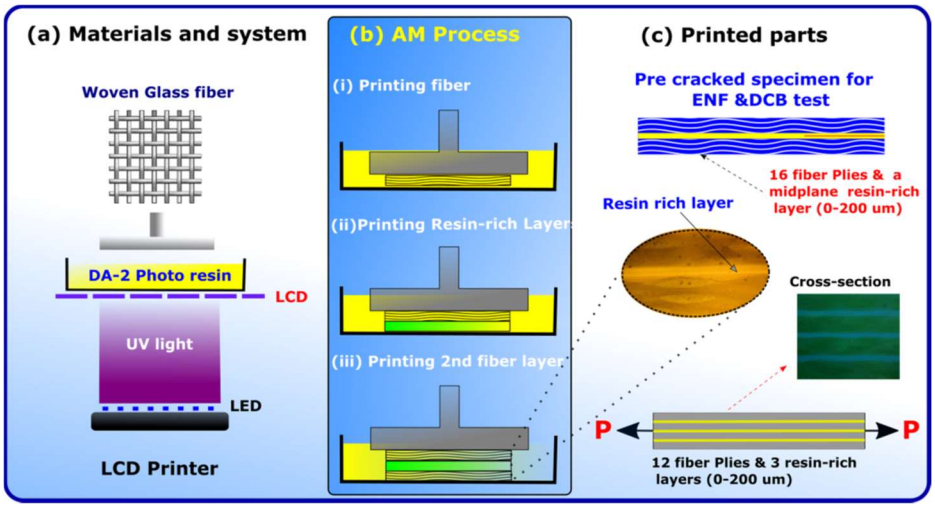

Figure 2. Diagram displaying resin-rich-layer technique on DLP printer [10].

Liquid deposition modeling is a non-vat method for resin 3D printing which cures photopolymer resin as it leaves an FDM-style deposition nozzle. This can be combined with continuous fiber for the printing of fiber-reinforced resins, and was tested to determine the influence of the selected resin on composite properties by Rahman et al. [11]. This experiment utilized several off-the-shelf UV resins with an added thermal initiator for an

additional curing method and was extruded through a custom nozzle for implementing the fiber tow through the extrusion, where it was cured by UV lasers upon exiting the nozzle. The thermal initiator was used with a heat cycle after printing for a post-cure. Samples with unidirectional reinforcement were printed for density ASTM D792, burn off ASTM D3171, tensile ASTM D3039, and flexural ASTM D7264 properties. Differential scanning calorimetry was performed to test for uncured resin, with computed tomography (CT) scanning performed to measure void content.

2.2.2. Multiple Resins

Multiple resin composites were typically manufactured with methods similar to inkjet printing, either with multiple nozzles or with a singular nozzle, referred to as direct ink writing. Articles repeatedly dealt with the flow characteristics of the uncured resin as differing resin rheology has a large impact on the difficulty to consistently deposit resins with the precision and consistency required for quality printing. These differing resins were commonly intended for utilizing differences in cured resin rigidity so that end items could be manufactured with combinations of flexible and rigid polymers.

Mixing requirements are explored by Ortega et al. [12], with the utilization of inks highly filled with BaSO4 or stainless steel (SS) particles being mixed into an unfilled ink during deposition shown in Figure 3. Cylindrical or grooved impellers described in Figure 4 are utilized for printing samples which are cut and imaged perpendicular to the extrusion path, with the fraction of mixing determined based on the percentage that is darkened with filler, as shown below.

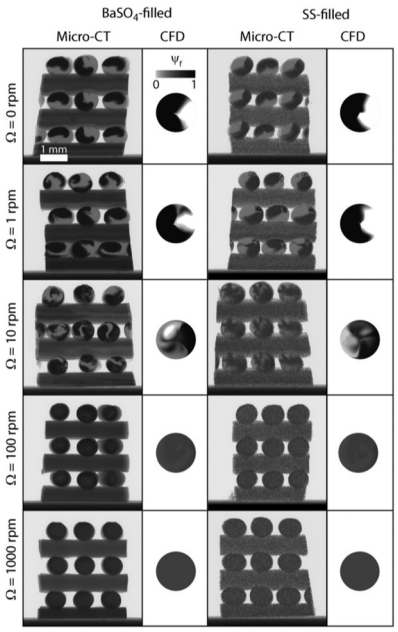

Figure 3. Cross-sectional images of ink displaying mixing completion of additive into matrix polymer [12].

The gating of material is studied by Scott et al. [13] for the switching of deposited resins through the same nozzle without mixing. The group printed transparent nozzles which are supplied through a path from each resin supply; this was observed for backflow and mixing of the active fluid into the static fluid supply. A model for Herschel–Bulkley fluids was developed for calculating maximum flow rates based on the path geometries described in Figure 5 and the resin rheology; from this, the asymmetric resin paths shown in Figure 6 were made, increasing the length of the path for thinner resins so that the resins would have similar flow rates.

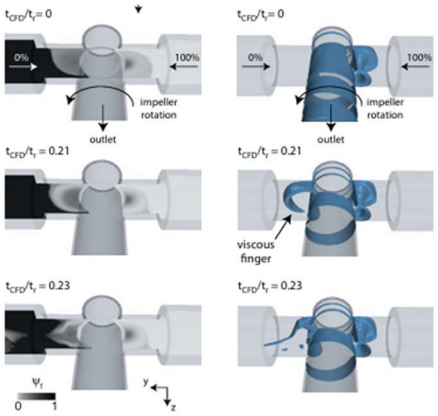

Figure 4. Diagram displaying fluid movement in mixing nozzle [12].

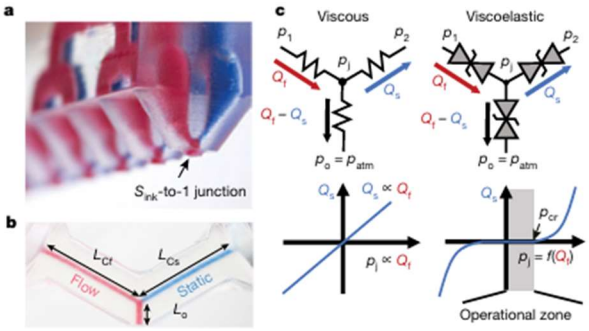

Figure 5. Resistance modeling diagrams for fluid flow. (**a**) Image of nozzles used. (**b**) Image displaying active and inactive fluid paths. (**c**) Resistance diagrams [13].

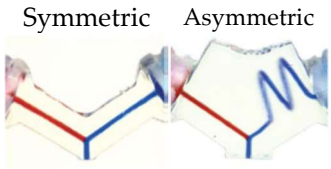

Figure 6. Comparison of resin channels after asymmetric modification to design flow resistance [13].

Table 1. Common additive manufacturing materials and reinforcements for research.

Method	Matrix	Reinforcements	Research Goal(s)	Citation
FDM	ABS	Epoxy CF—continuous CF—chopped GF—chopped Jute—chopped TiO_2 TPE MI, SS, Br, Cu, Bi, W	Structural reinforcement, Warpage reduction	[14–22]
FDM	PLA	Cellulose (Wood Fiber) CF—continuous CF—chopped Jute—continuous Silver–HNT HAP MI, SS, Br, Cu, Bi, W	Structural reinforcement, modulus control (mimic biological structures), antibacterial properties	[3,22–27]

Table 1. *Cont.*

Method	Matrix	Reinforcements	Research Goal(s)	Citation
FDM	PEI	CF—continuous CF—chopped	Structural reinforcement	[28–30]
FDM	PEEK	CF—chopped CF—continuous GF—continuous HAP	Structural reinforcement, modulus control (mimic biological structures), biocompatibility, electrical properties	[31–35]
FDM	PA	CF—continuous CF—chopped GF—continuous GF—chopped Kevlar—continuous Ceramic Fillers	Structural reinforcement, biocompatibility, wear resistance	[1,2,5,36–39]
Resin	Acrylate resins (PMMA, HDMMA, PPO, UDA)	GF—mat CF—continuous CF—chopped CGBs CF—nanotubes Graphene Oxide TiO_2 PEEK	Structural reinforcement, radar interaction effects, antibacterial properties	[8–11,18,40–43]
Resin	Epoxy, Resorcinol	CF—continuous GF—chopped NF—chopped PF—chopped Ink BMIMBF4 CF—nanotubes	Structural reinforcement, chemical reinforcement, viscosity, analysis/modeling, soft robotics, sensors	[4,6,13,44,45]
Resin	Silicone	Ink Silver (Ag) Graphene coating Carbon Grease Silica CF—continuous Kevlar—continuous Hemp fibers—chopped	Analysis/modeling, sensors, structural reinforcement	[13,46–51]
Resin	Siloxane (PDMS)	BaSO4, SS	Analysis/modeling	[12]

Acronyms in Table 1 not previously used: Hexanediol Dimethacrylate (HDMMA), Phenylbis Phosphine Oxide (PPO), nylon fiber (NF), polyester fiber (PF), Coated Glass Beads (CGBs), Urethane Diacrylate (UDA), Polydimethysylsiloxane (PDMS), 1-butyl-3-methylimidazolium tetrafluoroborate (BMIMBF4), Thermoplastic Elastomer (TPE), titanium dioxide (TiO_2), magnetic iron (MI), stainless steel (SS), bronze (Br), copper (Cu), bismuth (Bi), and tungsten (W).

2.3. Embedded Sensors

Methodology for embedded sensors is typically focused on utilizing a material with measurable electrical properties in conjunction with a material that is either non-invasive to the environments it will be utilized in, such as a glove, or a material that is well suited for use in another environment but has challenges with manufacturing control systems for such a device. These methods all involve soft compliant materials and sensing deformations in the system with changing resistivity. Almost all the reviewed articles utilized the findings to make a sensor that is applied to either biometrics or soft robotics.

Direct ink writing methods implementing ionogel ink into elastomers during mold setup are used by Truby et al. [49] to create sensors embedded within the end item, displayed in Figure 7. These sensors are based on resistive changes due to changing geometry curvatures, surface contact, and section inflation during deformation. These resistance

changes are tested in differing desired operating conditions of an effector for no-load and effector-applied varying force conditions, referred to as "dynamic free" and "blocked" movements. These values are further utilized in tests tugging on a ball from a gripper made and controlled in this manner, with the results from the sensors at different input conditions being recorded. Tests regarding temperature sensing were performed with the gripper and heated or cooled balls for resistive changes when gripping objects of differing temperatures. Finally, differing contact sensor designs were tested for differing surface depths.

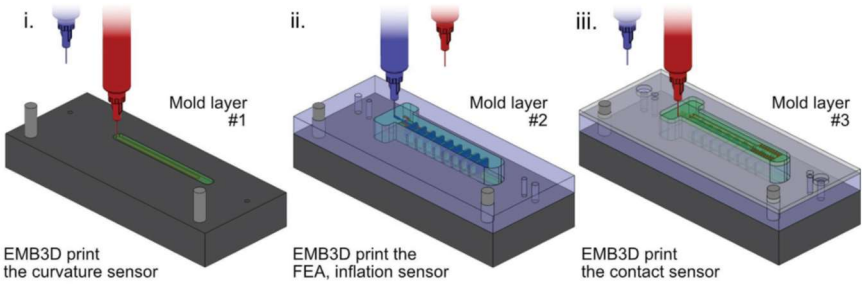

Figure 7. Diagram of direct ink writing into silicone mold [49].

Muth et al. [48] also utilized a direct ink writing method with carbon grease into an elastomer during molding. There was a focus on the rheological properties of the utilized elastomers and inks for design around printing machine parameters for the development of a reliable printing method. These were utilized to produce a soft sensing method embedded within the elastomer, measuring resistive changes in the ink when deformed. The ink deposition was varied with changes in nozzle size, extrusion pressure, and nozzle speed, which produced varying extrudate cross-section areas, which were tested to observe if smaller or larger areas produced larger changes in resistance upon deformation. The sensor resistances were checked for how consistent they were to original values. The sensors were stretched until mechanical failure, with resistances recorded for studying sensor performance up to failure. These were incorporated into a glove and measured for finger movement.

Ionogel inks for the direct writing method are explored as an alternative to gels with conductive fillers; specifically, shear thinning behaviors are investigated and designed for the development of an ionogel ink as desired properties for printing by Wong et al. [44]. The experiments demonstrated crosslinking in final curing and tested for tensile properties. Conductivity was measured both pre- and post-curing in addition to thermal stability testing. A voltage was applied across a sample during a set deflection cycle, with the current measured to demonstrate resistivity changes in the sample during deflection.

A nanocomposite ink was developed by Guo et al. [46] by utilizing silver nanoparticles designed around the utilization of the composite's conductive percolation threshold, varying dependent on strain. The varying percolation threshold values were utilized to create conductive inks that had minimal conductivity change during movement for electrodes by being past the percolation value, while also creating an ink at the percolation value so that tension or compression would produce a large change in conductivity for sensing. These inks were utilized along with non-conductive silicone and removable support material to produce sensors with the sensitive material between isolated electrodes. Sensor manufacturing is described in Figure 8. These sensors were tested at different pressures and frequencies for resistance changes and hysteresis. This sensor design was then applied on the skin above an artery for sensing blood pulse and printed onto a fingertip for testing durability before the production of an array of sensors for testing pressure mapping.

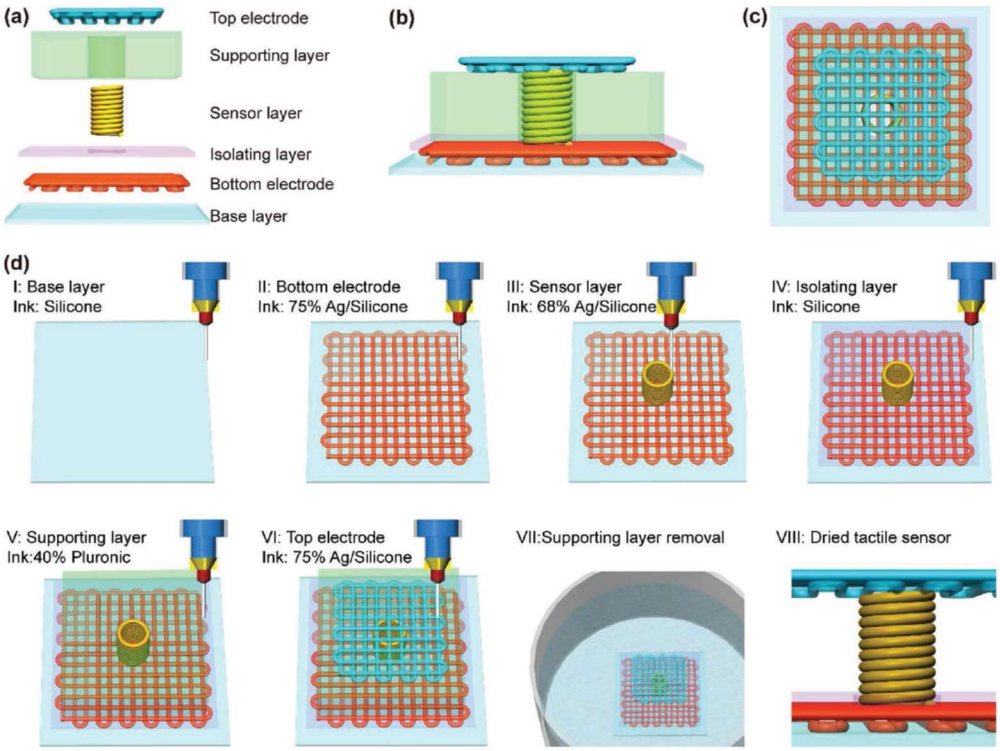

Figure 8. Diagram of process utilizing direct ink writing to build a tactile sensor with different inks. (**a**) Exploded view of each layer. (**b**) Diagram showing assembled layers. (**c**) Top view of assembled layers. (**d**) Progression through each layer deposition [46].

Nanoparticles were utilized by Davoodi et al. [47] to create a composite for biomonitoring via surface doping of substrates made with additively manufactured tooling. This was accomplished by coating the sacrificial molding with nanoparticles prior to molding, ensuring that the particles were integrated into the surface of the end item as opposed to a coating on the surface. Tests were performed to determine stability in regard to temperature, humidity, strain, solvents, and load cycling. Electrical resistivity was measured for different coating times, coating cycles, and nanoparticle concentrations in coating solution to determine the effects of this stage of manufacturing on the end item's properties and which values for each variable would be used for the experiment.

2.4. Medical

A silver antibacterial agent was vacuum-loaded into halloysite nanotubes (HNTs) for integration into UV resin for DLP processes by Sa et al. [27] for producing end items used in-mouth for dental care. Bending performance was tested by the ASTM D 793 standard; antibacterial property duration was tested with regularly changed artificial saliva which was then cultured to count colony-forming units; silver leeching was checked by measuring silver ion concentrations with flame spectrometry; and cytotoxicity was tested by cultured L929 cells further cultured in leaching solution.

Bone tissue scaffold composites were explored by Dubineko et al. [26] with varying poly-L-lactic acid (PPLA) and hydroxyapatite (HAp) mixes to control PLLA crystallinity for mimicking the Young's modulus of human bones. The PPLA and HAp were mixed via grinding of dried HAp in a ball mill, where PLLA was then dissolved into a solvent and mixed into the ball mill to be ground into the HAp. The mixture next had the solvent baked out of it; then, it was granulated and dried before being extruded into a filament suitable for FDM printing. This filament was used to produce test scaffolds, half of which were annealed. These samples were tested for deformation with additional thermogravimetric

analysis, differential scanning calorimetry, attenuated total reflectance Fourier transform infrared spectroscopy, SEM imaging, X-ray spectroscopy, and X-ray powder diffraction analysis, with nanoindentation for measuring Young's modulus.

3. Notable Additive Manufacturing Applications

3.1. Fiber-Reinforced FDM

The studies that focused on continuously reinforced polymers consistently showed that the 3D-printed continuous fibers, albeit also experiencing fiber breakage, still primarily failed through fiber pullout. The discontinuous fiber reinforcement showed significant improvements to unreinforced 3D prints but failed entirely through fiber pullout, and the comparisons showed an order of magnitude increase in strength along the fiber direction when using continuous fiber reinforcement. Several studies addressed the void content of 3D-printed composites in both continuous and discontinuous reinforcement, and it was noted that samples failed in a manner characteristic of poor void content.

Mohammadizedeh et al. [2] produced tensile, fatigue, and creep data regarding different infill patterns for continuous fiber reinforcements; they produced data for carbon fiber (CF), fiberglass (FG), and Kevlar fibers with concentric, isotropic, and combination concentric and isotropic infill patterns. This was accompanied by microstructure analysis detailing the failure methods at the microstructure level, which revealed that the primary fiber failure method was fiber pullout, shown in Figure 9.

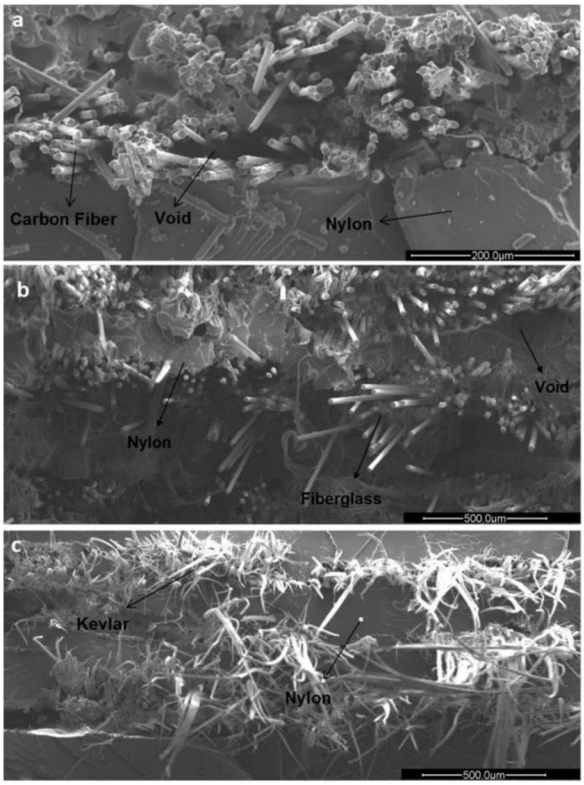

Figure 9. SEM images of sample fracture, with fiber pullout displayed. (**a**) Carbon fiber sample SEM. (**b**) Fiber-glass sample SEM. (**c**) Kevlar sample SEM [2].

Estakhrianhaghighi et al. [3] demonstrated changes to the strength of PLA with the inclusion of discontinuous wood fiber. These changes were primarily increases to the strength and toughness of the PLA; however, decreases after surpassing the ten-percent fiber weight content were noted to decrease mechanical strength. This decrease in higher-fiber-content samples is presumed to be caused by a lack of plasticizers improving polymer matrix wettability for the fiber; this lack of plasticizers makes the fiber mix with voids,

and after surpassing the ten-percent fiber weight, the void content was noted to increase dramatically. The thermal conductivity was noted to increase with depreciating returns after the void content began to increase.

The report by Blok et al. [1] includes an analysis of the macro-scale structure of the continuous and discontinuous fiber prints. This analysis includes a discussion regarding use cases of each, primarily the additional geometric constraints of continuous fibers and the difference in cost and time to produce additively manufactured continuous fibers compared to discontinuous fiber reinforcement. The results from the mechanical testing showed the continuous fiber reinforcement to be an order of magnitude greater than the strengths of the discontinuous reinforcement. The results from the testing were also analyzed and compared to trends in traditionally manufactured composites, with manufacturing flaws as follows: continuous fiber experienced stiffening, which is associated with wrinkled fibers breaking before better-aligned fibers can take a higher portion of load; continuous fibers had lower flexural strength than tensile strength and had compressive failures, both indicating poor void content and void-initiated failures; the short fiber did not reach the strength of the billet matrix material, indicating that none of the fibers reached fiber breakage before fiber pullout.

Zhang et al. [4] used their attempts to increase the fiber fraction to mitigate material weaknesses in open hole testing; the group was successful in utilizing the advantages of additive manufacturing, allowing for more control over the fiber direction so that stress could be directed around the hole in the sample, with large mechanical improvement over the typical composite drilled samples. This research also compared the failure methods in their samples with a lower void content to benchmark samples and found that their lower-void-content samples had breakages of the fibers as the primary failure method instead of fiber pullout, as shown in Figure 10.

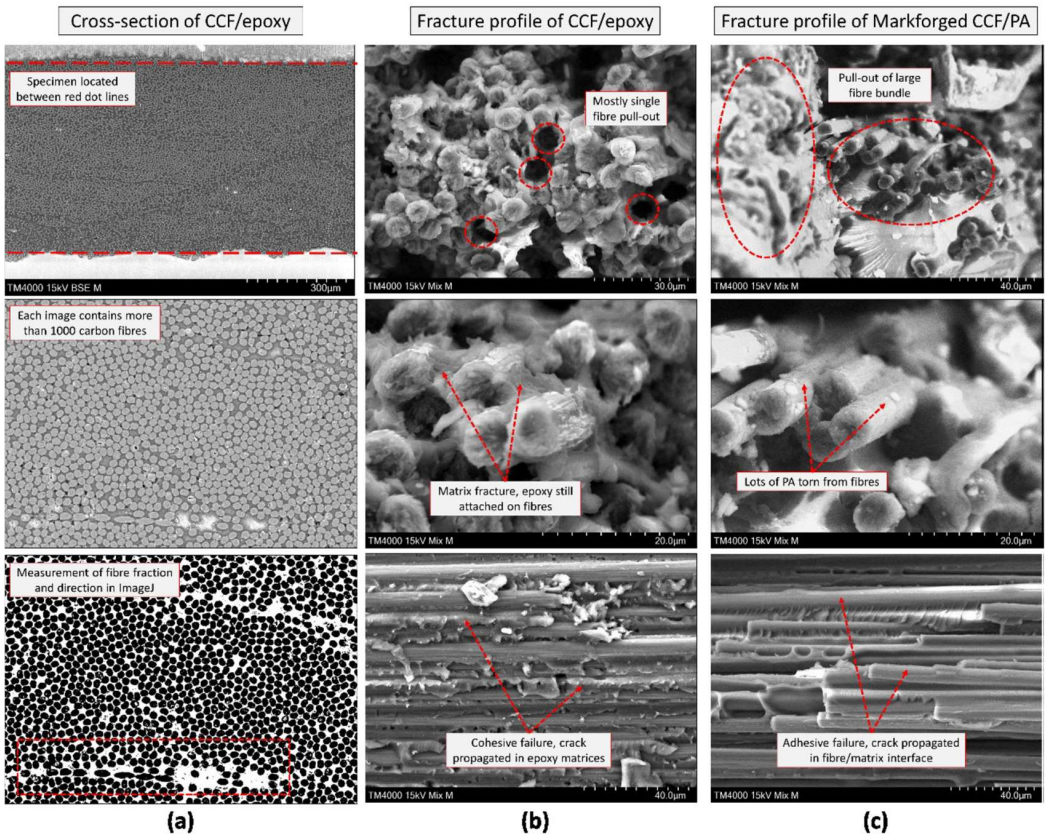

Figure 10. (**a**) SEM cross-sectional images of CF-reinforced resin; (**b**) SEM of fracture displaying voids from fiber pullout in CCF/Epoxy. (**c**) SEM of fracture displaying voids from fiber pull-out in CCF/PA [4].

The comparison to modeling attempts made by Abadi et al. [5] demonstrated that two typical modeling methods used to analyze traditionally manufactured composites were sufficient to describe the tested 3D-printed composite samples. The study also noted the impact of changing the fiber fraction to affect the resulting overall material properties by proportions close to the change in fiber fraction, with a 60% reduction in carbon fiber reducing the aligned modulus by 56%.

3.2. Resin

3.2.1. Reinforced Resin

Effects from reinforcement wetting were commonly found to affect the results of reviewed articles, with experiments that did not achieve expected wetting generally having mechanical properties lower than expected. The studies which had fiber tows exposed to a solvent wash before a post-cure generally showed poor fiber wetting, with one article specifically mentioning this as the suspected cause of poor wetting, whereas experiments that did not expose fiber tows to solvent had better wetting results.

The viscosity of UV resin was increased as the fiber content increased in Prashil et al. [6], which was the determining factor for which fiber contents would be easier to print, as lower viscosity was better for printing. The printed samples were characterized by hardness, gel content, water absorption, and chemical resistance. Fiberglass performed better in all mechanical evaluations, which is attributed to the lower chemical resistance of the compared fibers to the solvent used in resin production, resulting in less damage to the fiberglass. This is despite the fiberglass having the highest viscosity, which impeded processibility, and the worst dispersion of the tested fibers.

Fiber orientation effects from plate movement in vat photopolymerization were noted to have irregularities at the corners of rectangular build plates, indicating that a circular build plate would have material property improvements in Hofstatter et al. [7]. The fiber orientation was predicted to be parallel to the layer for bottom-up printing, with top-down printing adding a vertical alignment to the fibers through the z axis.

The samples modeled from naturally occurring fiber reinforcement in Khatua et al. [8] were not tested under a standardized testing method but were compared to unreinforced models with compression tests between two plates, which demonstrated an improved compression strength when reinforced with fibers. There was a noted decrease in stiffness with the fiber reinforcement despite the increase in strength, which prompted the utilization of a microscope to investigate the material failure; it was found that in the failed parts, the embedded fiber did not fully wet during printing. It was theorized that during post-processing, the print washing caused the ends of the fiber tows to allow washing away uncured impregnated resin before the post-cure.

Glass beads were found to increase the bending modulus but significantly lower the overall bending strength of samples in Gerbroodbar et al. [9]. The compression tests showed similar results with a higher modulus but a significant decrease in overall strength. The SEM analysis observed cavities formed by matrix–bead adhesion failure, initiating failure, as the beads would not deform or break under the stress before the adhesion would fail; this resulted in the load being transferred into a portion of the matrix that was unreinforced and with the voids from the beads further weakening the matrix.

Resin-rich layers were shown to be manufacturable by Idrees et al. [10] with additive manufacturing and are described as difficult to precisely manufacture with traditional methods. The resin-rich layers were shown to have a small increase in weight along with a decrease in modulus and stiffness; however, the testing showed improved properties relating to the damage tolerance of the composite.

Samples subjected to the dual-cure methods used by Rahman et al. [11] were shown to be fully cured after the post-processing heat cycle, and CT scanning showed a lack of void content between the fibers and matrix despite a notable void content between the deposited beads, which was indicated to be caused by the resin shrinkage during curing, and a model for predicting void content from the shrinkage rate was shown to be accurate. The samples printed were shown to have similar enough mechanical properties; the statistical analysis did not demonstrate significantly different performance along the fiber direction between the different resins used.

3.2.2. Multiple Resins

Critical values were typically found for achieving desired material behavior during processing, either mixing or non-mixing depending on the type of composite desired. These critical values were heavily influenced by the resin viscosities and path geometries.

A value was found for achieving full mixing of reinforced resin into unreinforced resin by Ortega et al. [12] followed by a computational modeling approach for predicting the critical rotational speed of a mixture achieving full mixing; this was followed by an analysis of the response time of the mixer to produce fully mixed extrudate.

Scott et al. [13] successfully created gating resistances with related fluid-mixing abbreviations for the utilized resins. This was patterned into a larger set of nozzles and utilized to manufacture soft robotics, with the separate rigid and elastic materials coupled to pneumatic controls for the demonstration of locomotion.

3.3. Embedded Sensors

The tested sensors were all found to successfully measure some combination of contact, pressure, and deflection. Most sensors were found to have minimal hysteresis in a use scenario, although some still showed hysteresis, often estimated as being from viscoelastic effects.

The combination of differing embedded sensors by Truby et al. [49] found combinations of distinct sensor values for differing operating conditions, which could be correlated to their associated conditions and utilized for control of soft robotics made from effectors, as tested. The test results included an investigation into the hysteresis behavior of the sensors and sensitivity to environmental conditions, finding minimal but present hysteresis in the sensors and a sensitivity to moisture over time. These results were found to be useful for feedback regarding the grip strength when holding a ball. Tests for sensing the temperature of the gripped objects found that there was a testable difference in resistances based on the gripped objects' temperature; however, these could not be differentiated from the pressure sensing in the tested embodiment. The differing contact sensor depths are correlated to changes in sensitivity at differing pressures.

Muth et al. [48] found that smaller ink cross-section areas have a larger change in resistance when deformed than a larger ink area has at the same strain values. Hysteresis observations were found to be significant, and estimations regarding the hysteresis source were made regarding the materials selected, with tests for the changes over cycle periods performed with large changes over the tested cycles. The sensors were found to have significantly differing resistances upon returning to original dimensions, albeit close to original values. The sensors performed well up until 400% strain and then gave values that were not consistent until mechanically failing via wire–sensor connection failure between 700 and 800% strain. The sensors embedded into a glove could successfully detect when fingers were opened or closed.

An ionogel that demonstrates rheological properties conducive to direct ink wringing was developed by Wong et al. [44]. The tensile properties were demonstrated in addition to experiments finding that crosslinking in the curing method reduced conductivity

by a third, which was noted as still being sufficient for the production of sensors. The change in resistivity was found to be consistent and predictable. The authors proceeded to demonstrate a sensor made by networking this material to be damage-tolerant due to the many conductive pathways shown in Figure 11, which is not a quality typically found in stretching sensors.

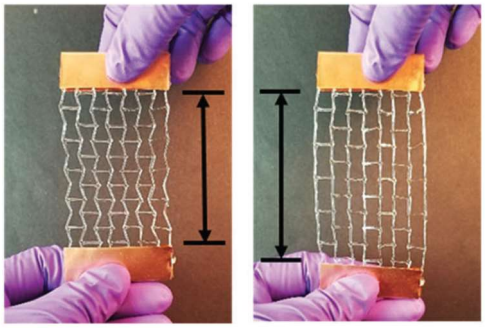

Figure 11. Stretchable sensor with multiple pathways shown elongating with stress between first and second image [44].

The nanocomposite ink from Guo et al. [46] was found to have silver particle contents that could provide drastic changes in conductivity, such as a 17,000% change or lesser changes, which was dialed in at 900% change for the same loads. Hysteresis was found at higher frequencies of load cycling; a significant change in resistance was also measured when applying different pressures. The sensors, when mounted to an artery, could measure heart rate, and could measure differences in values in pressure when conformally printed to a fingertip. The array tested could measure pressure from the shape of the supported object.

Davooli et al. [47] found that doping the surface of silicone with graphene nanoparticles produced a sensor that was very stable in solvents and differing humidities but had similar sensitivity to temperature as regularly coating the surface. This was integrated into a sensor pad integrated into a shoe and a pulse sensor strapped to a wrist over an artery; both of these sensors were utilized to demonstrate effective data collection and measuring of activity and pulse, respectively. Shrinkage effects on coating properties from silicone thinner loss during a processing step involving solvents are noted.

3.4. Medical

The flexural strength and modulus of the resin tested with Ag-HNT by Sa et al. [27] increased as Ag-HNT increased, pointing towards positive impacts on the mechanical properties. Cultures showed that antibacterial properties were retained at 7 days of exposure to artificial saliva. The silver ion concentration stayed higher than the 0.01 ppm minimum which will kill most bacteria; it was observed that a bubbling effect from the higher concentration of halloysite nanotubes in the 3% Ag-HNT sample caused the silver ion concentration for this sample to increase over time despite the opposite being typical. The cytotoxicity measured showed that the L929 cultures had a sufficiently unaltered growth rate; to conclude, the polymer is non-toxic.

Dubinenko et al. [26] found 50 wt% of HAp in annealed PLLA to mimic the properties of human bone; additionally, the HAp in the composite was found to have a large impact on the crystallinity of the PLLA of the composite. Young's modulus increased while crystallinity was noted to first decrease, then further decrease with annealing, and finally become more stable, with less change from annealing as the HAp content is increased. The mechanism of HAp in affecting crystallinity is presumed to be from exceeding the advantages of increased nucleation sites for crystal formation into filler concentrations that impede crystal formation on a molecular level.

4. Discussion

The high portion of fiber pullout failure in continuous fiber-reinforced FDM prints [2,4] is very interesting, since discontinuous fiber was shown to almost exclusively experience fiber pullout, and this was described as the reason why discontinuous fiber is so much weaker; the studies selected that tested continuous fiber consistently used materials and printers from Markforged, so it would be consistent for the continuous and discontinuous reinforced polymer comparisons to have also experienced significant fiber pullout. This leaves the presence of significantly fewer fibers in the continuous reinforcement as causing the most significant difference in strengths between continuous and discontinuous fibers, as otherwise, the increased adhesion surface would only result in a more linear increase in strength, dependent on the change in fiber length. Despite this, the study by Abadi et al. showed the fibers to overwhelmingly comprise the strength of the composite, which is what would be expected of a more typical composite that does not experience significant fiber pullout.

Discontinuously reinforced FDM polymers are shown to be drastically weaker than continuously reinforced FDM polymers. The studies that compare the two generally make a distinction between some differences in use case, primarily in the additional cost of design and production to achieve continuous fiber reinforcement in additive manufacturing compared to short fibers having comparatively little impact on the cost or time to implement compared to printing an unreinforced polymer.

The studies addressing void content typically note a high void content which increases as the fiber fraction is increased and is presumed to be due to processing fibers with a thicker thermoplastic matrix. The failure methods of samples are repeatedly noted as being typical of composites with poor void contents, evidenced, as shown by Zhang et al., to likely be a major factor in why tested samples do not reach the full strength of the fiber reinforcements used. There is a short comparison in Estakhrianhaghighi et al. between a commercial discontinuous reinforced polymer that contains a plasticizer compared to the produced samples which do not contain a plasticizer that theorizes a reduction in void content as positively impacting material properties.

One of the large advantages of a composite is the ability to tailor the material to the required properties and strengths; studies showing samples that follow expected modeling predictions of performance can help further the use of additive manufacturing in this regard. The anisotropic material properties of FDM printing when used with need-adjusted reinforcement can be an advantage for meeting material requirements within a geometry instead of the geometry-dependent material weakness that FDM is sometimes considered to have. The inherent aspect of FDM being a minimal tooling manufacturing method offers a high degree of geometric and toolpath customization for efforts in manufacturing and has the potential to offer more precise material property control when coupled with customized anisotropic material properties.

Additional research could be performed focusing on controlling void content to improve the utilization of the reinforcement's potential strength. The findings displaying the portion of strength that the reinforcement comprises and the failure methods observed would point towards controlling the void content as a prime area for improving the material properties of additively manufactured composites. This would also lead to notable studies regarding fatigue loading.

The observation of fiber wetting being removed by solvent washes was of particular note, as the study in question was the only one that did not feature increased stiffness from reinforcement. All other studies noted significant improvements in stiffness, including the study regarding the utilization of resin-rich layers to sacrifice stiffness improvements in favor of damage tolerance. The manufacture of fibers oriented as desired with the matrix

was treated in a more secondary manner as simply a means to manufacture the fiber as opposed to in FDM articles which did focus on fiber orientation, albeit within the confines of the desired matrix product.

Multiple-resin-printing research was typically focused on the control of the differing reinforced resins and their mixing instead of the resultant properties of the mixed resins. A large focus was placed on determining a method for both experimentally dialing in parameters and predicting a method for obtaining either a full mixture or full separation of the utilized resins. These studies seem geared towards the application of existing materials for implementation in manufacturing as a composite that leverages the advantages of each material by customizing the material properties at different locations in the print instead of optimizing the properties of the utilized materials themselves.

Resins have significant potential for future research which optimizes the properties of the utilized materials. It is notable to leverage the advantages already present to their maximum levels; however, new manufacturing methods can present an opportunity to improve those maxima. As more research is completed that opens the ability to leverage the advantages of more materials, the potential for improvements in material properties across more composite materials will be increased.

Research on embedded sensors was generally focused on a comparison to a similar manufacturing method for investigating improvements in how the items are currently made. The articles involving the development of a material often discussed the importance of the percolative electrical conductivity of a composite in material development, and how geometry changes during deflection will affect the values required for electrical conductivity network percolation. Direct ink writing is often the studied method for the delivery of silicone, as silicone has soft and biocompatible material properties which are useful for embedded sensor applications; the exception to utilizing direct ink writing was molding silicone. There is a large concern over signal hysteresis and stability in the presence of environmental factors; surface factors and nanocomposites played a larger role in this area of research than other applications of additively manufactured polymer composites.

5. Conclusions

A common theme among these research papers is the failure methods and what those mean for the impact to the material properties. Zhang et al. showed a direct comparison with samples produced with an epoxy and vacuum bagging, which did not suffer the same fiber pullout found in the benchmark continuous reinforced samples, similar to those used in other studies. This shows that there are still large improvements to be made even in continuous reinforcement methods before the maximum potential of the reinforcement can be realized. Despite this, if we assume that samples produced within the same proprietary and controlled ecosystem of Markforged's continuous fiber printing technology are comparable across studies, then the combination of studies reviewed would also demonstrate that the continuous fiber reinforcement already produces not only drastically higher improvements than discontinuous fibers but also the majority of the strength found in 3D-printed polymers, even though these samples suffer from a majority failure method of fiber pullout. These observations would be better reinforced within the course of a single study, but this is outside the scope of this review to perform.

The effect of fiber tows acting as routes for solvent washes to remove wetting would be a useful topic for a research article as it is currently evidenced but not directly experimented. The damage tolerance of resin-rich layers was also a notable article as it described 3D printing as the most effective method for manufacture and demonstrated advantages in lowering the primarily desired properties to preserve secondary required properties.

Multiple-resin printing focusing on the separation or mixing of the utilized resins points towards the increased difficulty of manufacturing with this method, as research is based on these parameters for getting the machines to work as intended, with the demonstrated examples having somewhat niche applications and tested material parameters, such as thermal conductivity or varying rigid and elastic use.

Funding: This research was funded by OUSD/R&E (The Under Secretary of Defense-Research and Engineering), National Defense Education Program (NDEP)/BA-1, Basic Research Via SMART Scholarship.

Data Availability Statement: The data that support the findings of this study are available from the corresponding author upon reasonable request.

Conflicts of Interest: The authors declare no conflicts of interest.

References

1. Blok, L.G.; Longana, M.L.; Yu, H.; Woods, B.K.S. An investigation into 3D printing of fibre reinforced thermoplastic composites. *Addit. Manuf.* **2018**, *22*, 176–186. [CrossRef]
2. Mohammadizadeh, M.; Imeri, A.; Fidan, I.; Elkelany, M. 3D printed fiber reinforced polymer composites—Structural analysis. *Compos. Part B* **2019**, *175*, 107112. [CrossRef]
3. Estakhrianhaghighi, E.; Mirabolghasemi, A.; Zhang, Y.; Lessard, L.; Akbarzadeh, A. 3D-Printed Wood-Fiber Reinforced Architected Cellular Composites. *Adv. Eng. Mater.* **2020**, *22*, 14. [CrossRef]
4. Zhang, H.; Zhang, K.; Li, A.; Wan, L.; Robert, C.; Brádaigh, C.M.; Yang, D. 3D printing of continuous carbon fibre reinforced powder-based epoxy composites. *Compos. Commun.* **2022**, *33*, 16. [CrossRef]
5. Al Abadi, H.; Thai, H.-T.; Paton-Cole, V.; Patel, V. Elastic properties of 3D printed fibre-reinforced structures. *Compos. Struct.* **2018**, *193*, 8–18. [CrossRef]
6. Desai, P.D.; Jagtap, R.N. Synthesis and Characterization of Fiber-Reinforced Resorcinol Epoxy Acrylate Applied to Stereolithography 3D Printing. *ACS Omega* **2021**, *10*, 31122–31131. [CrossRef]
7. Hofstätter, T.; Spangenberg, J.; Pedersen, D.B.; Tosello, G.; Hansen, H.N. Flow characteristics of a thermoset fiber composite photopolymer resin in a vat polymerization additive manufacturing process. *AIP Publ.* **2019**, *2065*, 020007. [CrossRef]
8. Khatua, V.; Gurumoorthy, B.; Ananthasuresh, G.K. Selectively embedding multiple spatially steered fibers in polymer composite parts made using vat photopolymerization. *arXiv* **2023**, arXiv:2303.15813. [CrossRef]
9. Gerdroodbar, A.E.; Alihemmati, H.; Zeighami, M.; Bodaghi, M.; Kouzani, A.Z.; Pourabbas, B.; Zolfagharian, A. Vat polymerization 3D printing of composite acrylate photopolymer-based coated glass beads. *Mater. Res. Express* **2023**, *10*, 085306. [CrossRef]
10. Idrees, M.; Ibrahim, A.M.; Tekerek, E.; Kontsos, A.; Palmese, G.R.; Alvarez, N.J. The effect of resin-rich layers on mechanical properties of 3D printed woven fiber-reinforced composites. *Compos. Part A* **2021**, *144*, 106339. [CrossRef]
11. Rahman, A.; Hall, E.; Gibbon, L.; Islam, Z.; Ulven, C.A.; La Scala, J.J. A Mechanical Performance Study of Dual Cured Thermoset Resin Systems 3D-Printed with Continuous Carbon Fiber Reinforcement. *Polymers* **2023**, *15*, 1384. [CrossRef] [PubMed]
12. Ortega, J.M.; Golobic, M.; Sain, J.D.; Lenhardt, J.M.; Wu, A.S.; Fisher, S.E.; Perez, L.X.P.; Jaycox, A.W.; Smay, J.E.; Duoss, E.B.; et al. Active Mixing of Disparate Inks for Multimaterial 3D Printing. *Adv. Mater. Technol.* **2019**, *4*, 13. [CrossRef]
13. Skylar-Scott, M.A.; Mueller, J.; Visser, C.W.; Lewis, J.A. Voxelated soft matter via multimaterial multinozzle 3D printing. *Nature* **2019**, *575*, 330–335. [CrossRef] [PubMed]
14. Belter, J.T.; Dollar, A.M. Strength of 3D Printed Fused Deposition Manufactured Parts Using the Fill Compositing Technique. *PLoS ONE* **2015**, *10*, e0122915. [CrossRef] [PubMed]
15. Mori, K.; Maeno, T.; Nakagawa, Y. Dieless forming of carbon fibre reinforced plastic parts using 3D printer. *Procedia Eng.* **2014**, *81*, 1595–1600. [CrossRef]
16. Zhong, W.; Li, F.; Zhang, Z.; Song, L.; Li, Z. Short fiber reinforced composites for fused deposition modeling. *Mater. Sci. Eng. A* **2001**, *301*, 125–130. [CrossRef]
17. Tekinalp, H.L.; Kunc, V.; Velez-Garcia, G.M.; Duty, C.E.; Love, L.J.; Naskar, A.K.; Blue, C.A.; Ozcan, S. Highly oriented carbon fiber–polymer composites via additive manufacturing. *Compos. Sci. Technol.* **2014**, *105*, 144–150. [CrossRef]
18. Ning, F.; Cong, W.; Qiu, J.; Wei, J.; Wang, S. Additive manufacturing of carbon fiber reinforced thermoplastic composites using fused deposition modeling. *Compos. Part B Eng.* **2015**, *80*, 369–378. [CrossRef]
19. Perez, A.R.T.; Roberson, D.A.; Wicker, R.B. Fracture Surface Analysis of 3D-Printed Tensile Specimens of Novel ABS-Based Materials. *J. Fail. Anal. Prev.* **2014**, *14*, 343–353. [CrossRef]

20. Torrado, A.R.; Shemelya, C.M.; English, J.D.; Lin, Y.; Wicker, R.B.; Roberson, D.A. Characterizing the effect of additives to ABS on the mechanical property anisotropy of specimens fabricated by material extrusion 3D printing. *Addit. Manuf.* **2015**, *6*, 16–29. [CrossRef]
21. Tsiakatouras, G.; Tsellou, E.; Stergiou, C. Comparative study on nanotubes reinforced with carbon filaments for the 3D printing of mechanical parts. *World Trans. Eng. Technol. Educ.* **2014**, *12*, 392–396.
22. Ranaiefar, M.; Singh, M.; Salem, J.A.; Halbig, M.C. Compressive Properties of Additively Manufactured Metal-Reinforced PLA and ABS Composites. *Polymers* **2024**, *16*, 2008. [CrossRef] [PubMed]
23. Li, N.; Li, Y.; Liu, S. Rapid prototyping of continuous carbon fiber reinforced polylactic acid composites by 3D printing. *J. Mater. Process. Technol.* **2016**, *238*, 218–225. [CrossRef]
24. Ferreira, R.T.L.; Amatte, I.C.; Dutra, T.A.; Bürger, D. Experimental characterization and micrography of 3D printed PLA and PLA reinforced with short carbon fibers. *Compos. Part B* **2017**, *124*, 88–100. [CrossRef]
25. Matsuzaki, R.; Ueda, M.; Namiki, M.; Jeong, T.-K.; Asahara, H.; Horiguchi, K.; Nakamura, T.; Todoroki, A.; Hirano, Y. Three-dimensional printing of continuous-fiber composites by in-nozzle impregnation. *Sci. Rep.* **2016**, *6*, 23058. [CrossRef] [PubMed]
26. Dubinenko, G.; Zinoviev, A.; Bolbasov, E.; Kozelskaya, A.; Shesterikov, E.; Novikov, V.; Tverdokhlebov, S. Highly filled poly(L-lactic acid)/hydroxyapatite composite for 3D printing of personalized bone tissue engineering scaffolds. *Appl. Polym. Sci.* **2020**, *138*, 10. [CrossRef]
27. Sa, L.; Kaiwu, L.; Shenggui, C.; Junzhong, Y.; Yongguang, J.; Lin, W.; Li, R. 3D printing dental composite resins with sustaining antibacterial ability. *Mater. Life Sci.* **2019**, *54*, 3309–3318. [CrossRef]
28. De Backer, W.; Bergs, A.P.; Van Tooren, M.J. *Multi-Axis Multi-Material Fused Filament Fabrication with Continuous Fiber Reinforcement*; Reston USA American Institute of Aeronautics and Astronautics: Reston, VA, USA, 2018.
29. Vakharia, V.S.; Leonard, H.; Singh, M.; Halbig, M.C. Multi-Material Additive Manufacturing of High Temperature Polyetherimide (PEI)–Based Polymer Systems for Lightweight Aerospace Applications. *Polymers* **2023**, *15*, 561. [CrossRef]
30. Chuang, K.C.; Grady, J.E.; Draper, R.D.; Shin ES, E.; Patterson, C.; Santelle, T.D. Additive Manufacturing and Characterization of Ultem Polymers and Composites. In *The Composites and Advanced Materials Expo CAMX*; NTRS.NASA: Dallas, TX, USA, 2015.
31. Stepashkin, A.A.; Chukov, D.; Senatov, F.; Salimon, A.; Korsunsky, A.; Kaloshkin, S. 3D-printed PEEK-carbon fiber (CF) composites: Structure and thermal properties. *Compos. Sci. Technol.* **2018**, *164*, 319–326. [CrossRef]
32. Vatandaş, B.B.; Uşun, A.; Yıldız, N.; Şimşek, C.; Cora, N.; Aslan, M.; Gümrük, R. Additive manufacturing of PEEK-based continuous fiber reinforced thermoplastic composites with high mechanical properties. *Compos. Part A* **2023**, *167*, 107434. [CrossRef]
33. Rodzeń, K.; Sharma, P.K.; McIlhagger, A.; Mokhtari, M.; Dave, F.; Tormey, D.; Sherlock, R.; Meenan, B.J.; Boyd, A. The Direct 3D Printing of Functional PEEK/Hydroxyapatite Composites via a Fused Filament Fabrication Approach. *Polymers* **2021**, *13*, 545. [CrossRef] [PubMed]
34. Rodzeń, K.; McIvor, M.J.; Sharma, P.K.; Acheson, J.G.; McIlhagger, A.; Mokhtari, M.; McFerran, A.; Ward, J.; Meenan, B.J.; Boyd, A.R. The Surface Characterisation of Fused Filament Fabricated (FFF) 3D Printed PEEK/Hydroxyapatite Composites. *Polymers* **2021**, *13*, 3117. [CrossRef] [PubMed]
35. Liu, X.; Shan, Z.; Liu, J.; Xia, H.; Ao, X.; Zou, A.; Wu, S. Mechanical and electrical properties of additive manufactured high-performance continuous glass fiber reinforced PEEK composites. *Compos. Part B* **2022**, *247*, 110292. [CrossRef]
36. Van Der Klift, F.; Koga, Y.; Todoroki, A.; Ueda, M.; Hirano, Y.; Matsuzaki, R. 3D Printing of Continuous Carbon Fibre Reinforced Thermo-Plastic (CFRTP) Tensile Test Specimens. *Open J. Compos. Mater.* **2016**, *6*, 18–27. [CrossRef]
37. Nakonieczny, D.S.; Kern, F.; Dufner, L.; Antonowicz, M.; Matus, K. Alumina and Zirconia-Reinforced Polyamide PA-12 Composites for Biomedical Additive Manufacturing. *Materials* **2021**, *14*, 6201. [CrossRef] [PubMed]
38. Abderrafai, Y.; Mahdavi, M.H.; Sosa-Rey, F.; Hérard, C.; Navas, I.O.; Piccirelli, N.; Lévesque, M.; Therriault, D. Additive manufacturing of short carbon fiber-reinforced polyamide composites by fused filament fabrication: Formulation, manufacturing and characterization. *Mater. Des.* **2022**, *214*, 110358. [CrossRef]
39. Bolat, Ç.; Ergene, B. Wear performance of short fiber added polyamide composites produced by additive manufacturing: Combined impacts of secondary heat treatment, reinforcement type, and test force. *Polym. Compos.* **2024**, *45*, 6885–6900. [CrossRef]
40. Zhang, Y.; Li, H.; Yang, X.; Zhang, T.; Zhu, K.; Si, W.; Liu, Z.; Sun, H. Additive manufacturing of carbon nanotube-photopolymer composite radar absorbing materials. *Polym. Compos.* **2016**, *39*, E671–E676. [CrossRef]
41. Lin, D.; Jin, S.; Zhang, F.; Wang, C.; Wang, Y.; Zhou, C.; Cheng, G.J. 3D stereolithography printing of graphene oxide reinforced complex architectures. *Nanotechnology* **2015**, *26*, 434003. [CrossRef] [PubMed]
42. Yugang, D.; Yuan, Z.; Yiping, T.; Dichen, L. Nano-TiO_2-modified photosensitive resin for RP. *Rapid Prototyp. J.* **2011**, *17*, 247–252. [CrossRef]
43. Chen, S.-G.; Yang, J.; Jia, Y.-G.; Lu, B.; Ren, L. TiO_2 and PEEK Reinforced 3D Printing PMMA Composite Resin for Dental Denture Base Applications. *Nanomaterials* **2019**, *9*, 1049. [CrossRef]

44. Wong, J.; Gong, A.T.; Defnet, P.A.; Meabe, L.; Beauchamp, B.; Sweet, R.M.; Sardon, H.; Cobb, C.L.; Nelson, A. 3D Printing Ionogel Auxetic Frameworks for Stretchable Sensors. *Adv. Mater. Technol.* **2019**, *4*, 6. [CrossRef]
45. Sandoval, J.H.; Wicker, R.B. Functionalizing stereolithography resins: Effects of dispersed multi-walled carbon nanotubes on physical properties. *Rapid Prototyp. J.* **2006**, *12*, 292–303. [CrossRef]
46. Guo, S.-Z.; Qiu, K.; Meng, F.; Park, S.H.; McAlpine, M.C. 3D Printed Stretchable Tactile Sensors. *Adv. Mater.* **2017**, *29*, 1701218. [CrossRef] [PubMed]
47. Davoodi, E.; Montazerian, H.; Haghniaz, R.; Rashidi, A.; Ahadian, S.; Sheikhi, A.; Chen, J.; Khademhosseini, A.; Milani, A.S.; Hoorfar, M.; et al. 3D-Printed Ultra-Robust Surface-Doped Porous Silicone Sensors for Wearable Biomonitoring. *ACS Nano* **2020**, *14*, 1520–1532. [CrossRef]
48. Muth, J.T.; Vogt, D.M.; Truby, R.L.; Mengüç, Y.; Kolesky, D.B.; Wood, R.J.; Lewis, J.A. Embedded 3D Printing of Strain Sensors within Highly Stretchable Elastomers. *Adv. Mater.* **2014**, *26*, 6307–6312. [CrossRef]
49. Truby, R.L.; Wehner, M.; Grosskopf, A.K.; Vogt, D.M.; Uzel, S.G.M.; Wood, R.J.; Lewis, J.A. Soft Somatosensitive Actuators via Embedded 3D Printing. *Adv. Mater.* **2018**, *30*, e1706383. [CrossRef] [PubMed]
50. Liu, W.; Peeke, L.M.; Periyasamy, M.; Campbell, R.R.; Hickner, M.A. Additive manufacturing of silicone composite structureswith continuous carbon fiber reinforcement. *Polym. Eng. Sci.* **2023**, *63*, 1716–1724. [CrossRef]
51. Koushki, P.; Kwok, T.-H.; Hof, L.; Wuthrich, R. Reinforcing silicone with hemp fiber for additive manufacturing. *Compos. Sci. Technol.* **2020**, *194*, 108139. [CrossRef]

Disclaimer/Publisher's Note: The statements, opinions and data contained in all publications are solely those of the individual author(s) and contributor(s) and not of MDPI and/or the editor(s). MDPI and/or the editor(s) disclaim responsibility for any injury to people or property resulting from any ideas, methods, instructions or products referred to in the content.